COMMONWEALTH OF KENTUCKY

BEFORE THE PUBLIC SERVICE COMMISSION

In the Matters of:

ELECTRONIC APPLICATION OF KENTUCKY UTILITIES COMPANY FOR AN ADJUSTMENT OF ITS ELECTRIC RATES, A CERTIFICATE OF PUBLIC CONVENIENCE AND NECESSITY TO DEPLOY ADVANCED METERING INFRASTRUCTURE, APPROVAL OF CERTAIN REGULATORY AND ACCOUNTING TREATMENTS, AND ESTABLISHMENT OF A ONE-YEAR SURCREDIT	)	CASE NO. 2020-00349
ELECTRONIC APPLICATION OF LOUISVILLE GAS AND ELECTRIC COMPANY FOR AN ADJUSTMENT OF ITS ELECTRIC AND GAS RATES, A CERTIFICATE OF PUBLIC CONVENIENCE AND NECESSITY TO DEPLOY ADVANCED METERING INFRASTRUCTURE, APPROVAL OF CERTAIN REGULATORY AND ACCOUNTING TREATMENTS, AND ESTABLISHMENT OF A ONE-YEAR SURCREDIT	)	CASE NO. 2020-00350

KENTUCKY SOLAR INDUSTRIES ASSOCIATION, INC.
RESPONSE TO KENTUCKY PUBLIC SERVICE COMMISSION
STAFF'S THIRD DATA REQUESTS

Comes now the Kentucky Solar Industries Association, Inc. (KYSEIA), by and through counsel, and submits its combined responses to Commission Staff's Third Data Requests.

Respectfully submitted,

/s/David E. Spenard
Randal A. Strobo
Clay A. Barkley
David E. Spenard
STROBO BARKLEY PLLC
730 West Main Street, Suite 202
Louisville, Kentucky 40202
Phone: 502-290-9751
Facsimile: 502-378-5395
Email: rstrobo@strobobarkley.com
Email: cbarkley@strobobarkley.com
Email: dspenard@strobobarkley.com
Counsel for KYSEIA

NOTICE AND CERTIFICATION FOR FILING

Undersigned counsel provides notice that the electronic version of the paper has been submitted to the Commission by uploading it using the Commission's E-Filing System on this 2nd day of August 2021, and further certifies that the electronic version of the paper is a true and accurate copy of each paper filed in paper medium. Pursuant to the Commission's March 16, 2020, March 24, 2020, and July 22, 2021 Orders in Case No. 2020-00085, *Electronic Emergency Docket Related to the Novel Coronavirus Covid-19*, the paper, in paper medium, is not required to be filed.

/s/ David E. Spenard
David E. Spenard

NOTICE REGARDING SERVICE

The Commission has not yet excused any party from electronic filing procedures for this case.

/s/ David. E. Spenard
David E. Spenard

Kentucky Solar Industries Association, Inc.
KY PSC Case No. 2020-00349 and
Case No. 2020-00350
Response to Commission Staff's Third Data Requests

Witnesses Responsible:
Justin R. Barnes

1. Refer to the Supplemental Testimony of Justin R. Barnes (Supplemental Barnes Testimony), page 9, lines 13–15. Provide supporting calculation of the proposed capacity rate of $0.0357/kWh in Excel spreadsheet format with all formulas, columns, and rows unprotected and fully accessible.

Response:

Please see Mr. Barnes' workpapers, which are attached. The tab labeled ELCC LOLP – DST contains calculations underlying the hourly LOLP weighting and ELCC calculation. The raw hourly LOLP data was sourced from:

https://psc.ky.gov/pscecf/2020-00349/rick.lovekamp%40lge-ku.com/04012021020836/2020_PSC_DR5_KU_Attach_to_Q19_-_DER_LOLP_EUE.xlsx

The tab labeled Gen Capacity shows the calculation of capacity value. Capacity costs are based on the PJM Net CONE in terms of UCAP $/MW-day for the most recent three auction years.

Kentucky Solar Industries Association, Inc.
KY PSC Case No. 2020-00349 and
Case No. 2020-00350
Response to Commission Staff Third Data Requests

Witnesses Responsible:
Justin R. Barnes

2. Refer to the Supplemental Barnes Testimony, page 10, lines 18–20.

a. Provide supporting calculation of the proposed avoided transmission cost rate of $0.01989/kWh and $0.01037/kWh for KU and LG&E, respectively, under the loss of load probability methodology in Excel spreadsheet format with all formulas, columns, and rows unprotected and fully accessible.
b. Provide supporting calculation of the proposed avoided transmission cost rate of $0.00812/kWh and $0.00782/kWh for KU and LG&E, respectively, under the 6 coincident peak methodology in Excel spreadsheet format with all formulas, columns, and rows unprotected and fully accessible.

Response:

a. Please see Mr. Barnes' workpapers, which are attached. The transmission unit costs were derived from:

Kentucky Utilities: https://psc.ky.gov/pscecf/2020-00349/mike.hornung%40lge-ku.com/01222021020208/2020_AG-KIUC_DR1_KU_Attach_to_Q188_-_Att_3_KU_LOLP_COSS_with_Unit_Costs.xlsx

Louisville Gas & Electric: https://psc.ky.gov/pscecf/2020-00350/rick.lovekamp%40lge-ku.com/01222021013405/2020_AG-KIUC_DR1_LGE_Attach_to_Q188_-_att_3_LGE_LOLP_COSS_with_Unit_Costs.xlsx

b. Please see Mr. Barnes' workpapers, which are attached. The 6CP hours used to calculate effective solar capacity under a 6CP scenario are sourced from: https://psc.ky.gov/pscecf/2020-00349/rick.lovekamp%40lge-ku.com/04122021030810/2020_Rebuttal_Testimony_Seelye_Workpapers_-_KU_LGE_Residential_Class_Shapes_20210326.xlsx

The transmission unit costs for the 6CP scenario were derived from:

Kentucky Utilities: https://psc.ky.gov/pscecf/2020-00349/mike.hornung%40lge-ku.com/01222021020208/2020_AG-KIUC_DR1_KU_Attach_to_Q188_-_Att_1_KU_6CP_COSS_with_Unit_Costs.xlsx

Louisville Gas & Electric: https://psc.ky.gov/pscecf/2020-00350/rick.lovekamp%40lge-ku.com/01222021013405/2020_AG-KIUC_DR1_LGE_Attach_to_Q188_-_att_1_LGE_6CP_COSS_with_Unit_Costs.xlsx

Kentucky Solar Industries Association, Inc.
KY PSC Case No. 2020-00349 and
Case No. 2020-00350
Response to Commission Staff Third Data Requests

Witnesses Responsible:
Justin R. Barnes

3. Provide all utilities that have used a loss of load probability (LOLP) or similar approach for estimating avoided transmission and distribution capacity costs.

Response:

Mr. Barnes is not aware of any other utility that has used this approach, but the Minnesota Value of Solar Methodology uses the same ELCC for calculating both avoided generation capacity and transmission. To be clear, the LOLP data is simply used for defining the effective capacity provided by solar during peak hours.

The lack of utility examples for the use of LOLP for assigning peak capacity contributions is attributable to the fact that few, if any, other utilities use LOLP in the assignment of demand-related production costs in their cost of service study. More commonly, demand-related production costs would be allocated based on a coincident peak allocator (e.g., 1CP, 6CP) or an energy-weighted coincident peak allocator (e.g., 4CP average and excess). Transmission cost responsibility typically also uses a coincident peak allocator, often the same allocator as is used for production capacity, because both types of costs are driven by system peak demand. Mr. Barnes elected to use an ELCC derived from LOLP for transmission to reflect the common practice of using the same allocator for both transmission and generation demand-related costs. Accordingly, since the Companies use LOLP production capacity allocation, the same measure of contribution to peak was used for transmission.

For the purpose of clarity, for distribution costs, Mr. Barnes did not recommend the use of LOLP to determine the solar capacity contribution for calculating avoided distribution costs. Specifically, Mr. Barnes' Supplemental Testimony stated:

"I recommend that the effective capacity contribution for the purposes of distribution costs be based on expected solar production during a rate class's highest load hours. For that purpose, I recommend that the calculation be made for hours where the class load is within 10% of the maximum hourly class load. For instance, if maximum class load during any hour was 2,000 MW, the calculation would use all hours where class load was greater than 1,800 MW."

The effective solar capacity in this instance would not be based on high-LOLP hours. Rather, the hours would correspond to those hours of the highest maximum demand for a given class, as maximum class demand is commonly used for allocation of demand-related distribution costs.

Kentucky Solar Industries Association, Inc.
KY PSC Case No. 2020-00349 and
Case No. 2020-00350
Response to Commission Staff Third Data Requests

Witnesses Responsible:
Justin R. Barnes

4. According to the references listed below, an approach to calculating the effective load carrying capacity (ELCC) transforms the LOLP into a loss of load expectation (LOLE). Explain why Mr. Barnes relied on the LOLP approach as opposed to the LOLE approach.

   • NREL, Determining the Capacity Value of Wind: An Updated Survey of Methods and Implementation, 2008.
   • PJM, Effective Load Carrying Capability (ELCC), 2020.
   • NREL, Estimating the Costs and Benefits of Avoided Generation Capacity, 2014.
   • CPUC, Decision (D.) 19-09-043, issued under Rulemaking (R.) 18- 07-003 on October 3rd, 2019.
   • NREL, Methods for Analyzing the Benefits and Costs of Distributed Photovoltaic Generation to the U.S. Electric Utility System.

Response:

Calculating ELCC based on a target LOLE requires complex system modeling to identify how incremental amounts of capacity affect achievement of a target LOLE. The complexities are discussed at some length in the 2008 NREL report referenced in this inquiry, as are a series of simpler methods.

Mr. Barnes' method of performing a simplified solar capacity contribution calculation is equivalent to the Capacity Factor Approximation method identified in:

Madaeni, S.H.; Sioshansi, R.; Denholm, P. (2012). Comparison of Capacity Value Metrics for Photovoltaics in the Western United States. NREL Report No. NREL/TP-6A20-54704. Golden CO: National Renewable Energy Laboratory.

Link: https://www.nrel.gov/docs/fy12osti/54704.pdf
(And attached to this response.)

This method uses a single set of LOLPs and weights each hour according to the sum of LOLPs for the number of hours used in the calculation. Mr. Barnes' calculation uses the full set of hours with a non-zero LOLP, though the approximation may use a different number of hours (e.g., top 10, top 100). This report found that the Capacity Approximation Method produced results for solar capacity contribution closest to a full iterative ELCC-based approach for a sample of systems that were under study (using the top 10 LOLP hours). Mr. Barnes elected to use the full number of non-zero LOLP hours in his calculation to avoid the need to make a subjective judgment on the proper

set of “high” LOLP hours to include. A smaller set of hours would likely produce a higher ELCC result because the highest LOLP hours generally align with early to mid-afternoon hours.

NREL
NATIONAL RENEWABLE ENERGY LABORATORY

Comparison of Capacity Value Methods for Photovoltaics in the Western United States

Seyed Hossein Madaeni and
Ramteen Sioshansi
The Ohio State University

Paul Denholm
National Renewable Energy Laboratory

NREL is a national laboratory of the U.S. Department of Energy, Office of Energy Efficiency & Renewable Energy, operated by the Alliance for Sustainable Energy, LLC.

Technical Report
NREL/TP-6A20-54704
July 2012

Contract No. DE-AC36-08GO28308

NREL
NATIONAL RENEWABLE ENERGY LABORATORY

Comparison of Capacity Value Methods for Photovoltaics in the Western United States

Seyed Hossein Madaeni and Ramteen Sioshansi
The Ohio State University

Paul Denholm
National Renewable Energy Laboratory

Prepared under Task No. SS12.2210

National Renewable Energy Laboratory
15013 Denver West Parkway
Golden, Colorado 80401
303-275-3000 • www.nrel.gov

Technical Report
NREL/TP-6A20-54704
July 2012

Contract No. DE-AC36-08GO28308

NOTICE

Available electronically at http://www.osti.gov/bridge

Available for a processing fee to U.S. Department of Energy
and its contractors, in paper, from:

U.S. Department of Energy
Office of Scientific and Technical Information
P.O. Box 62
Oak Ridge, TN 37831-0062
phone: 865.576.8401
fax: 865.576.5728
email: mailto:reports@adonis.osti.gov

Available for sale to the public, in paper, from:

U.S. Department of Commerce
National Technical Information Service
5285 Port Royal Road
Springfield, VA 22161
phone: 800.553.6847
fax: 703.605.6900
email: orders@ntis.fedworld.gov
online ordering: http://www.ntis.gov/help/ordermethods.aspx

Cover Photos: (left to right) PIX 16416, PIX 17423, PIX 16560, PIX 17613, PIX 17436, PIX 17721

Printed on paper containing at least 50% wastepaper, including 10% post consumer waste.

Acknowledgments

The authors would like to thank Venkat Banunarayanan, Dr. Chris Dent, Trieu Mai, Michael Milligan, and Robin Newmark for helpful discussions and suggestions.

Abstract

This report compares different capacity value estimation techniques applied to solar photovoltaics (PV). It compares more robust data and computationally intense reliability-based capacity valuation techniques to simpler approximation techniques at 14 different locations in the western United States. The capacity values at these locations are computed while holding the underlying power system characteristics fixed. This allows the effect of differences in solar availability patterns on the capacity value of PV to be directly ascertained, without differences in the power system confounding the results. Finally, it examines the effects of different PV configurations, including varying the orientation of a fixed-axis system and installing single- and double-axis tracking systems, on the capacity value. The capacity value estimations are done over an eight-year running from 1998 to 2005, and both long-term average capacity values and interannual capacity value differences (due to interannual differences in solar resource availability) are estimated. Overall, under the assumptions used in the analysis, we find that some approximation techniques can yield similar results to reliability-based methods such as effective load carrying capability.

Table of Contents

List of Figures

List of Tables

1 Introduction

An important aspect of the benefits of renewable electricity is its capacity value, or the ability of renewable generators to reliably meet demand. Generator outages, which can occur due to mechanical failures, planned maintenance, or lack of real-time generating resources (especially in the case of renewables), may leave a power system with insufficient generating capacity to meet load. According to the North American Electric Reliability Corporation (NERC), quantifying the contribution of renewable energy resources to resource adequacy of bulk power systems is a very important and emerging issue [1]. Therefore, assessing the adequacy of renewable generation technologies and consequently estimating their capacity value is crucial for accurate reliability and planning of power systems [2]. Previous analyses have considered the capacity value of wind [1, 3–8], photovoltaic (PV) solar [9–14], and concentrating solar power (CSP) plants [15]. Partially due its maturity, the capacity value of wind has been more widely studied than solar technologies.

This report expands on previous PV analyses and details techniques that can be used to estimate the capacity value of PV plants using historical data. The techniques consist of reliability and statistical methods used to estimate the probability of a system outage event and the contribution of PV in reducing this probability. The primary purpose of this report is to provide a comprehensive comparison of different capacity value estimation techniques. Specifically, it compares more robust data and computationally intense reliability-based capacity valuation techniques to simpler approximation techniques. It compares these methods at 14 different locations in the western United States. The capacity values at these locations are computed while holding the underlying power system characteristics fixed. This allows the effect of differences in solar availability patterns on the capacity value of PV to be directly ascertained, without differences in the power system confounding the results. Finally, it examines the effects of different PV configurations, including varying the orientation of a fixed-axis system and installing single- and double-axis tracking systems, on the capacity value. The capacity value estimations are done over an eight-year running from 1998 to 2005, and both long-term average capacity values and interannual capacity value differences (due to interannual differences in solar resource availability) are estimated. The capacity values are all computed for small (100 MW) PV installations. Therefore, the estimates are for marginal PV installations and do not account for the diminishing marginal capacity value of PV that will occur with higher PV penetrations. Moreover, the capacity values at the different locations are computed in isolation, thus the capacity values do not account for the effect of spatial correlation of solar availability on capacity values.

2 Methods For Estimating Capacity Value

Methods for estimating the capacity value of renewable resources can be categorized in two major classes. These differ in terms of computational complexity and data requirements. The first class uses reliability-based methods and includes equivalent conventional power (ECP), effective load carrying capability (ELCC), and equivalent firm capacity (EFC). These methods use power system reliability evaluation techniques [16], which are based on loss of load probability (LOLP) and loss of load expectation (LOLE). LOLP is defined as the probability of a loss of load event in which the system load is greater than available generating capacity during a given time period. LOLP is typically computed in one-hour increments. The LOLE is the sum of the LOLPs during a planning period—typically one year. LOLE gives the expected number of time periods in which a loss of load event occurs.[1] Power system planners typically aim to maintain an LOLE value of 0.1 days/year (or 2.4 hours per year based on the target of one outage-day every 10 years) [17]. This value is used as the target LOLE value throughout this report. Reliability methods are widely accepted and considered accurate methods for calculating capacity value [5–8]. A second

Defining Capacity-Related Terms

This report focuses on the capacity value of PV plants. There are a number of capacity-related terms commonly used with substantially different meanings.

Capacity generally refers to the rated output of the plant when operating at maximum output. Capacity is typically measured in terms of a kilowatt (kW), megawatt (MW), or gigawatt (GW) rating. Rated capacity may also be referred to as "nameplate capacity" or "peak capacity." This may be further distinguished as the "net capacity" of the plant after plant parasitic loads have been considered, which are subtracted from the "gross capacity."

AC versus DC capacity. PV modules produce direct current (DC) voltage. This DC electricity is converted into alternating current (AC). As a result, PV power plants have both a DC rating (corresponding to the output of the modules) and an AC rating, which is always lower than the DC rating considering the various losses associated with converting DC to AC. This analysis uses the AC rating, which better corresponds to traditional power plant capacity ratings.

Capacity factor is a measure of how much energy is produced by a plant compared to its maximum output. It is measured as a percentage, generally by dividing the total energy produced during some period of time by the amount of energy it would have produced if it ran at full output over that period of time.

Capacity value is the focus of this report and refers to the contribution of a power plant to reliably meeting demand. Capacity value is the contribution that a plant makes toward the planning reserve margin, with a more comprehensive technical definition provided in Section 2. The capacity value (or capacity credit) is measured either in terms of physical capacity (kW, MW, or GW) or the fraction of its nameplate capacity (%). Thus, a plant with a nameplate capacity of 150 MW could have a capacity value of 75 MW or 50%. Solar plants can be designed and operated to increase their capacity value or energy output.

Capacity payment is a monetary payment to a generator based on its capacity. The capacity payment is generally in terms of $/MW where the MW is the amount of capacity sold into the market.

[1] This also may consider the need to import electricity. For example an International Energy Agency document describes a "risk level" as "a probability of the power system under investigation not to be able to cover its peak demand without electricity import. Here 'without import into the system' needs to be highlighted. It means that the criteria not being met do not automatically lead to a blackout in the system. Instead, cross border transit capacities have to be used in a fact that links adequacy to market and regulatory aspects" [18].

class of methods uses approximations that are simpler but vary in accuracy, especially for variable generation. These methods include Garver's ELCC approximation [19], Z method [20], and capacity factor-based methods [21].

Conventional generator outages are typically modeled using an equivalent forced outage rate (EFOR), which is the probability that a particular generator can experience a failure at any given time. When renewables are added to a system, the system reliability models must also capture the variability of real-time resource availability. To do this, renewable resource availability is typically estimated using historical data or by simulating such data.

The following sections discuss common techniques for estimating capacity value of renewable and conventional generators in greater detail.

2.1 Equivalent Conventional Power

One of the most robust and widely accepted definitions of capacity value is the ECP of a generator. The ECP of a generator is defined as the amount of a different generating technology that can replace the new generator while maintaining the same system reliability level [7]. In the context of a renewable generator, this is attractive because it allows the capacity value of a renewable generator to be measured in terms of a conventional dispatchable generator.

The steps used to calculate the ECP of a PV generator[2] are as follows:

1. For a given set of conventional generators, the LOLE of the system without the PV plant is calculated as:

$$LOLE = \sum_{i=1}^{T} P(G_i < L_i) \qquad (1)$$

where T is the total number of hours of study, G_i represents the available conventional capacity in hour i, and L_i is the amount of load. $P(G_i < L_i)$ indicates the probability of available generating capacity being less than demand, which is the LOLP in each hour. Adding these LOLPs together gives the LOLE. The calculated LOLE will represent the original reliability level of the system. In order to meet the standard planning target of one outage-day every 10 years [17], we adjust the loads in each hour so the LOLE of the base system, given by equation (1) is 0.1 days/year. This load adjustment is done by applying a fixed percentage change to each hourly load, with the load adjustments ranging between 0.1% and 5% between the different study years.

2. The PV plant is added to the system and the new LOLE, which is denoted $LOLE_{PV}$, is calculated as:

$$LOLE_{PV} = \sum_{i=1}^{T} P(G_i + C_i < L_i) \qquad (2)$$

[2] This method can be applied to any generating resource, including non-PV renewables. This is done by substituting the candidate generator, for which the ECP is being calculated, in place of the PV plant.

where C_i denotes the output of the PV plant in hour i. Since the PV plant has been added to the system, $LOLE_{PV}$ will be lower than the LOLE of the base system (indicating a more reliable system with lower LOLPs).

3. The PV plant is "removed" from the system and a conventional generator is added. The LOLE of the new system, which is denoted as $LOLE_{Gen}$ is computed as:

$$LOLE_{Gen} = \sum_{i=1}^{T} P(G_i + X_i < L_i) \qquad (3)$$

where X_i is the available generating capacity in hour i from the added conventional generator. This added conventional generator is assumed to have a fixed EFOR, but the nameplate capacity of the plant is adjusted until the LOLE of the system with the PV plant and the conventional generator are equal (i.e., until $LOLE_{PV} = LOLE_{Gen}$). The nameplate capacity of the conventional generator that achieves this equality is defined as the ECP of the PV plant. We assume that the benchmark generator to which the PV plant is compared is a natural gas-fired combustion turbine because such generators are often built for peak capacity purposes. The ECP of the PV plant will be sensitive to this assumption because different generation technologies against which it could be benchmarked will have different EFORs.

2.2 Effective Load Carrying Capability

The ELCC of a generator is defined as the amount by which the system's loads can increase (when the generator is added to the system) while maintaining the same system reliability (as measured by the LOLP and LOLE) [7]. The steps used to calculate the ELCC of a PV generator[3] are as follows:

1. For a given set of conventional generators, the LOLE of the system without the PV plant is calculated using equation (1).
2. The PV plant is added to the system and the LOLE is recalculated. This is shown in (2). Again, $LOLE_{PV}$ will be lower than the LOLE of the base system because we have added generation to the system.
3. Keeping the PV plant in the system a constant load is added in each hour. The LOLE of the new system, which is denoted as $LOLE_{Load}$ is computed as:

$$LOLE_{Load} = \sum_{i=1}^{T} P(G_i < L_i + D) \qquad (4)$$

where D is the load added in each hour. The value of D is adjusted until the LOLEs calculated in steps 1 and 3 (i.e., the LOLE of the base system and the system with the added PV and load) equal each other. The value of D that achieves this equality is defined as the ELCC of the PV plant.

2.3 Equivalent Firm Capacity

The EFC of a generator is defined as the amount of a different fully reliable generating technology (i.e., a generator with an EFOR of 0%) that can replace the new generator while

[3] As with ECP, this method can be applied to any generating resource, including non-PV renewables. This is done by substituting the candidate generator, for which the ELCC is being calculated, in place of the PV plant.

maintaining the same system reliability level [7, 22–23]. The steps used to calculate the EFC of a PV generator[4] are as follows:

1. For a given set of conventional generators, the LOLE of the system without the PV plant is calculated using equation (1).
2. The PV plant is added to the system and the LOLE of the system, which is denoted $LOLE_{PV}$, is calculated according to (2).
3. The PV plant is "removed" from the system and a fully reliable conventional generator (EFOR of 0%) is added. The LOLE of the new system, which is denoted as $LOLE_{Gen}$ is computed according to (3) with the difference that X_i is the available generating capacity in hour i from the added fully reliable conventional generator.
4. The nameplate capacity of the plant is adjusted until the LOLE of the system with the PV plant and the conventional generator are equal (i.e., until $LOLE_{PV} = LOLE_{Gen}$). The nameplate capacity of the conventional generator that achieves this equality is defined as the EFC of the PV plant. Note that a generator's EFC and ELCC will generally differ because changing the generation mix of a system will change the distribution of the available capacity in a given hour whereas adjusting loads will not [6].

Reliability-based methods, such as ECP, ELCC, and EFC, require detailed system data, including EFORs of all of the generators in the system, generator capacities, and loads. Moreover, due to seasonal and annual weather pattern changes, one will typically need several years' worth of data to accurately estimate the capacity value of any type of renewable generation technology including PV.

2.4 Approximation Methods

Computational challenges associated with full reliability-based calculations have led to the development of approximation techniques. These techniques often require less data and analytical effort and are typically used by utilities and system operators for capacity planning purposes [1]. These approximation methods reduce the computational burden by focusing on the hours in which the system faces a high risk of not meeting load—typically hours with high loads or LOLPs. While ignoring transmission constraints reduces the computational burden both from an operational and reliability perspective, iterative calculation of LOLE in the ELCC and ECP methods still requires extensive calculations. Several studies have compared the accuracy of approximation methods and reliability-based approaches, such as the ELCC method, for calculating capacity value of wind and CSP. For example, Bernow et al. [24] and El-Sayed [25] estimate the capacity value of a wind plant by considering only the peak-load hours. They use the average capacity factor of wind during peak-load hours, defined as the actual output of the plant during those hours divided by its nameplate capacity, as a proxy for the capacity value. Milligan and Parsons [21] calculate the capacity value of wind by considering a set of "risky" hours, as opposed to only peak-load hours. They introduce three different techniques, which will be explained in Section 2.4.1. They recommend using the top 10% of hours for proper approximation of capacity value. In a similar study Madaeni et. al. [15] have applied the same techniques to CSP plants and found that only considering the top 10 hours is sufficient for a

[4] As with ECP and ELCC, this method can be applied to any generating resource, including non-PV renewables. This is done by substituting the candidate generator, for which the EFC is being calculated, in place of the PV plant.

reasonable approximation of capacity value. This is due to stronger correlation between CSP and loads.

The following sections describe some of these approximation techniques in further detail. Note that all of these techniques are intended to approximate a generator's ELCC. In Section 5.2, we explicitly compare the accuracy of these methods to the ELCC method.

2.4.1 Capacity Factor Approximation Method

A common approximation technique considers the capacity factor of a generator over a subset of periods during which the system faces a high risk of an outage event. These techniques have been applied to wind [24–25] and PV [9] and compared with reliability-based methods to assess their accuracy. Milligan and Parsons [21] introduce three different approximation methods, which differ based on the set of hours examined. One technique uses the average capacity factor during the peak-load hours, whereas another uses the capacity factor during the peak-LOLP hours. A third technique uses the highest-load hours but normalizes the capacity factors by the LOLPs. This technique places higher weight on the capacity factor of the wind plant during hours with high LOLPs. Milligan and Parsons have applied these techniques to the top 1% to 30% of hours and have shown that the approximation can approach the ELCC metric if a suitable number of hours is considered. Their results suggest that using the top 10% of hours is typically sufficient. In this report we use the third technique to approximate the capacity value of PV. Henceforth we will refer to this technique as CF approximation.

The intuition behind the weighting in CF approximation is that the capacity provided by the PV is especially needed during hours with higher LOLPs. The weights are obtained as:

$$w_i = \frac{LOLP_i}{\sum_{j=1}^{T} LOLP_j} \qquad (5)$$

where w_i is the weight in hour i, $LOLP_i$ is the LOLP in hour i, and T is the number of hours in the study. These weights are then used to calculate the weighted average capacity factor of the PV plant in the highest-load hours as:

$$CV = \sum_{i=1}^{T'} w_i C_i \qquad (6)$$

where T' is the number of hours used in the approximation and CV is the weighted generation of the PV plant during the high-load hours and is considered as an approximation for capacity value.

2.4.2 Garver's Approximation Method

Garver proposes an approximation for the full ELCC calculation [19], which Hoff et al. [10] use to determine the capacity value of PV. The aim of Garver's method is to quantify ELCC without needing to recalculate LOLEs when the new generator is added to the system. This dramatically reduces the computational burden because it does not require iterative LOLE calculations to achieve the equality between the LOLEs computed in steps 2 and 3 of the ELCC method.

Garver's method uses a linearized risk function to relate the LOLE of a system to its excess generation capacity when plotted on a logarithmic basis. The slope of this risk function, *m*, represents the necessary capacity for an annual LOLE that is *e* times greater than the original LOLE.

Garver's method approximates the ELCC of a PV plant by first estimating the LOLE of the system when the PV plant is added as:

$$\sum_{i=1}^{T} exp\left(\frac{-(PL - L_i + C_i)}{m}\right) \qquad (7)$$

where *PL* is the annual peak load, L_i is the hourly load, and C_i is the hourly PV output. If we substitute the output of the PV plant with a constant, denoted *ELCC*, the system LOLE would change to:

$$\sum_{i=1}^{T} exp\left(\frac{-(PL - L_i + ELCC)}{m}\right) \qquad (8)$$

The ELCC approximation is given by the value of *ELCC*, which yields equality between equations (7) and (8). A closed-form solution for the value of *ELCC* is given by:

$$\text{ELCC} = \text{m} \times Ln\left[\frac{\sum_{i=1}^{T} exp\left(\frac{-(PL - L_i)}{m}\right)}{\sum_{i=1}^{T} exp\left(\frac{-(PL - L_i + C_i)}{m}\right)}\right] \qquad (9)$$

Henceforth this method is denoted as GA.

2.4.3 Garver's Approximation Method for Multi-State Units

D'Annunzio and Santoso [26] generalize Garver's approximation method to model multi-state generators. This can include conventional generators that can experience different outage states (e.g., operating at reduced capacity due to an outage) or renewables, which can operate at reduced capacity due to resource availability. The methodology has two main assumptions:

1. The probability distribution of renewable availability remains the same in different time periods.
2. The LOLE of a system can be approximated as Be^{md}, where *d* as the annual peak load and *B* and *m* are parameters. These parameters can be estimated by estimating the LOLE of the system using equation (1) with different system peaks (e.g., by increasing all loads proportionally) and fitting values for *B* and *m* to the LOLE values.

Their method approximates the ELCC of a generator as:

$$ELCC = -\frac{1}{m} \times Ln\left[\sum_{i=1}^{T} p_i e^{-mC_i}\right] \qquad (10)$$

where P_i is the probability of the PV plant to generate C_i. In this report we consider an empirical probability distribution for PV generation. The empirical distribution that we consider assigns probabilities P_i to each generating state C_i by counting the number of occurrences of C_i divided by the total number of hours used in the analysis. We also construct the distribution with a certain resolution defined as the number of megawatts between two generating states. The lower the resolution the more accurate the PV is modeled. While we conduct our analysis based on an empirical distribution with 1 MW resolution, we further study the sensitivity of the method with respect to changes in the resolution. Henceforth this technique will be referred to as GAM.

2.4.4 Z Method

The Z method [20] considers the difference between available generating capacity and load in peak hours as a random variable, *S*, with a Gaussian distribution and assuming small additional PV capacity [27]. The z statistic for this random variable, defined as mean divided by standard deviation, is considered to be a reliability metric of the power system. This is shown in equation (11) where μ_s and σ_s refer to the mean and standard deviation of *S*.

$$z_0 = \frac{\mu_s}{\sigma_s} \qquad (11)$$

The Z method is based on the major assumption that the shape of probability distribution of *S* does not change when a new generator is added to the system, although the mean and variance of the distribution can change.

Assuming that the above assumption holds, the ELCC of a new generator can be defined as the amount of incremental load that keeps the z statistic constant after the addition of that generator to the system. Reference [20] elaborates on the derivations required to reach to a closed form solution, which approximates ELCC based on the above assumption. We only provide the closed form solution here, which is shown in (12) where $\bar{\mu}_{PV}$ and $\bar{\sigma}_{PV}$ are mean and standard deviation of PV availability.

$$ELCC = \bar{\mu}_{PV} - \frac{z_0 \bar{\sigma}_{PV}^2}{2\sigma_s} \qquad (12)$$

The Z method is only valid when its underlying assumption is satisfied. For small PV penetration this will not be an issue. However, as penetration increases, the shape of distribution for surplus is subject to change and therefore the method will no longer be valid.

2.5 Comparison of Reliability-Based Methods and Approximation Techniques

Each of the methods described in Section 2 differ in terms of computational burden. Table 1 summarizes and contrasts the requirements of each technique. Additional comparison and discussion of the applicability of several of these different methods is provided by Zachary and Dent [27].

Table 1. Comparison Between Reliability-Based Methods and Approximation Techniques for Quantifying Capacity Value

Method	Type	Computational Burden	Data Requirements
Equivalent Conventional Power (ECP)	Relia.	High—LOLPs have to be iteratively computed to achieve equality between LOLEs when PV and benchmark units are added	Load and generator capacities and EFORs
Effective Load-Carrying Capability (ELCC)	Relia.	High—LOLPs have to be iteratively computed to achieve equality between LOLEs when PV and load are added	Load and generator capacities and EFORs
Equivalent Firm Capacity (EFC)	Relia.	High—LOLPs have to be iteratively computed to achieve equality between LOLEs when PV and perfectly reliability benchmark unit are added	Load and generator capacities and EFORs
Capacity Factor-Based Approximation (CF)	Approx.	Low—At most, LOLPs must be computed once, if highest-LOLP or LOLP-weighted methods are used	Loads only for highest-load method, otherwise generator capacities and EFORs
Garver's ELCC Approximation (GA)	Approx.	Medium—LOLPs must be computed a handful of times to estimate the slope of the risk function	Load and generator capacities and EFORs
Garver's Approximation for Multi-State Units (GAM)	Approx.	Medium—LOLPs must be computed a handful of times to estimate the relationship between LOLE and system peak	Load and generator capacities and EFORs
Z Method	Approx.	Low—The mean and standard deviation of the surplus of the system without PV and output of the PV must be computed	Load and generator capacities and EFORs

3 Photovoltaic Model

This study uses PV generation profiles produced by the National Renewable Energy Laboratory's System Advisor Model (SAM) [28].[5] SAM is a software platform capable of simulating dynamics of solar resources, including PV. Historical weather data are input to SAM in order to simulate hourly electrical output of the PV plant. These generation profiles are then used as inputs for the capacity valuation methods discussed in Section 2. For the purposes of estimating capacity values, we assume the base PV plant has a nameplate capacity of 100 MW-DC. This corresponds to an AC capacity of 83.4 MW under standard test conditions (STC), which are 1,000 W/m^2 of solar irradiation and a cell temperature of 25^{o}C [28]. This AC rating is used to normalize the capacity values we estimate throughout the report. Note that the AC capacity under STC is not necessarily the maximum AC capacity of the plant. There could be conditions wherein the PV plant generates more than 83.4 MW, which would yield a capacity value of more than 100%. The assumption of a 100 MW-DC PV plant implies that this analysis only considers the capacity value of adding a small 'marginal' amount of PV to the system. This study does not consider the effect of higher PV penetrations on reducing the marginal capacity value of additional PV.

SAM includes four different PV performance models [28]. Our analysis is based on the California Energy Commission model. Inverter characteristics are based on the Sandia Inverter Performance model (SIPM). These inverters have a non-linear behavior, making them significantly more efficient at high power outputs.[6] Figure 1 illustrates the efficiency of the inverter under different operating conditions.[7]

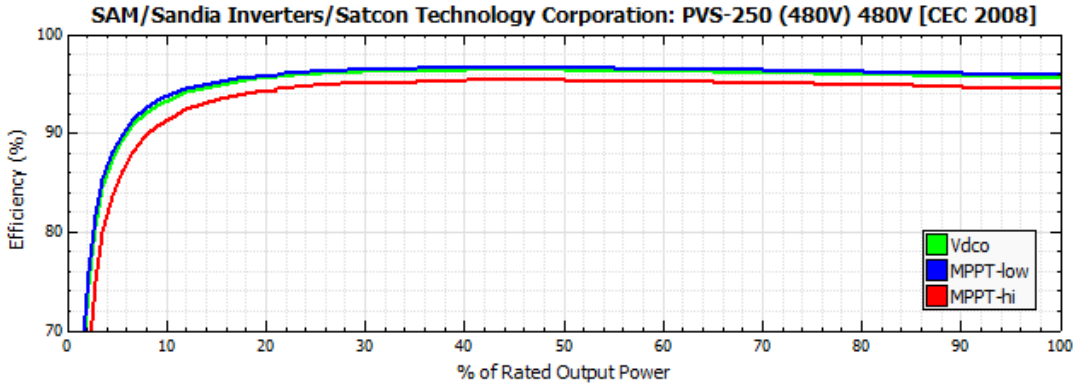

Figure 1. Inverter efficiency curve[8]

[5] SAM is available for download at https://sam.nrel.gov/. This analysis was conducted with version 2011.6.30.
[6] The base inverter type used is the Satcon Technology Corporation PVS-250. Results are fairly insensitive to different inverters offered by other manufacturers. We compared the total annual generation of a fixed-axis PV plant located in Bartsow, California (coordinates in Table 3) with three additional inverters (Eaton SM1003, Kacon New Energy Blue Planet XP 100U, and Xantrex Technologies GT 100.) The maximum change in the generation profile was less than 0.6%.
[7] Where MPPT-low corresponds to manufacture specified minimum DC operating voltage, MPPT-hi corresponds to manufacture-specified maximum DC operating voltage and Vdco corresponds to the average of MPPT-low and MTTP-hi.
[8] Derived from the SAM model documentation in version 2011.6.30.

4 Data Requirements

This study focuses on the sites in the western United States listed in Table 2. These sites were chosen to represent a mix of locations across the western U.S. with at least one of two key characteristics: relatively good solar resource or within urban areas. PV in urban areas can be attractive because transmission capacity might not be available to transfer power from areas with relatively high solar resource. Moreover, rooftop PV can be more easily deployed in populated areas.

All of the PV sites that we model are in the Western Interconnection, which we refer to here as the Western Electricity Coordinating Council (WECC) region.[9] This analysis uses the entire WECC footprint to determine system loads and LOLPs. Because this assumption keeps the underlying system fixed, **differences in the capacity value of PV at different locations can be attributed entirely to differences in solar resource**, without system characteristics confounding the results. This essentially assumes utilities have the ability to share capacity resources across the entire Western Interconnect. Utilities and system planners typically use a smaller footprint because they are primarily interested in ensuring reliability within the limited territory that they serve. Thus, the capacity values reported here can be different from such an analysis. This is because PV output may be more or less coincident with the 'local' load of a more limited system than it is with the WECC-wide load. Previous analyses of PV have tended to use more limited system footprints as well and have in some cases shown differences in capacity values that stem from coincidence between PV output and the local load [29].

Table 2. Location of PV Plants

PV Site	Coordinates	Characteristic
Bartsow, CA	35.15° N, 117.35° W	High Solar Resource
Congress, AZ	34.15° N, 113.15° W	High Solar Resource
Yucca Flat, NV	37.25° N, 116.15° W	High Solar Resource
Hanover, NM	33.05° N, 107.75° W	High Solar Resource
Cheyenne, WY	41.35° N, 104.95° W	Urban Area
Salt Lake City, UT	41.05° N, 112.05° W	Urban Area
Boise, ID	43.85° N, 116.25° W	Urban Area
Los Angeles, CA	34.45° N, 118.45° W	Urban Area
San Francisco, CA	37.85° N, 122.45° W	Urban Area
Seattle, WA	47.75° N, 122.45° W	Urban Area
Denver, CO	39.95° N, 104.85° W	Urban Area
Albuquerque, NM	35.25° N, 106.65° W	Urban Area
Phoenix, AZ	33.45° N, 111.95° W	Urban Area
Las Vegas, NV	36.25° N, 115.15° W	Urban Area

The ECP and ELCC metrics, along with approximation techniques described in Section 2.4, are used to estimate the capacity value of the PV plant during the years 1998–2005. Data requirements and sources used for this analysis are listed below.

[9] The Western Interconnection is one of the three U.S. interconnected grids and is largely isolated from the other two interconnects—ERCOT and the Eastern Interconnect.

1. Conventional generator data

    A. This analysis uses the rated capacity and EFOR of each generator in the WECC region. The rated capacities are obtained from Form 860 (Annual Electric Generator Report) data filed with the U.S. Department of Energy's Energy Information Administration (EIA) [30]. The EIA data specifies a winter and summer capacity, which capture the effect of ambient temperature on the maximum operating point of thermal generators. The EIA data also specify the prime mover and generating fuel of each generator. These data are combined with the NERC's Generating Availability Data System (GADS) to estimate the EFOR of each generator [31]. The GADS data give historical average EFORs for generators based on generating capacity and technology.

    B. The conventional generator used as the benchmark unit in the ECP calculation is a natural-gas-fired combustion turbine with an EFOR of 7%, which is based on the EFOR reported in GADS.

2. Hourly load data

    A. Hourly historical WECC load data for the years 1998–2005 are obtained from Form 714 filings with the Federal Energy Regulatory Commission (FERC) [32]. The FERC data includes load reports for nearly all of the load-serving entities (LSEs) and utilities in the WECC, although some smaller municipalities and cooperatives are not reflected in the data.

3. PV generation profile

    A. In order to provide the most robust capacity value estimates, multiple years of PV generation data is needed. Because no PV plants are operating at the exact study locations, we model the operation of a PV plant using SAM. As part of input data for SAM, hourly weather data for each location are obtained from the National Solar Radiation Data Base.[10]

[10] These data are available for download at http://rredc.nrel.gov/solar/old_data/nsrdb/.

5 Capacity Value of Photovoltaic Solar Plants

This section details results regarding the capacity value of a 100 MW-DC PV located at the sites listed in Table 2 and illustrated in Figure 2. All capacity values are normalized by the 83.4 MW-AC capacity of the plant under STC. We examine systems with different sun-tracking capabilities. For PV arrays with fixed axis, arrays are set to face south with a tilt angle equal to the site's latitude.[11] Changing the orientation (facing east, south, or west) or the tilt angle of such PV systems can affect capacity value. This is due to the fact that different orientations will favor either morning or afternoon production. An analysis of the effects of PV orientation for such systems, including the optimal orientation in terms of energy yield and capacity value, is provided in Section 6.1. For PV systems with single-axis tracking, the tilt angle is set to 0, meaning that the array is completely horizontal but it rotates about the azimuth angle in order to follow daily movement of the sun. For PV systems with double-axis tracking the array rotates about both azimuth and tilt angles to follow daily and seasonal movement of the sun.

5.1 Capacity Value of Photovoltaic Power using Reliability-Based Methods

Two different reliability-based techniques, ECP and ELCC, are used to determine the capacity value of PV. Capacity values are estimated for fixed-axis, single-axis, and double-axis tracking PVs. Table 3 summarizes average capacity values over the eight years of study using ECP and ELCC. An intuitive finding is that capacity values are highest for double-axis tracking PVs. Moreover, Table 3 reveals that ELCCs are less than ECPs. This is because when calculating ECP, PV is benchmarked against a fictitious generator with a positive EFOR, which we assume to be 7%. With ELCC, on the other hand, PV is compared to a constant load, which is akin to a fully reliable generator with an EFOR of 0. Hence a PV plant would have a lower capacity value when compared to a fully reliable generator, as shown in Table 3.

Depending on the location and the sun-tracking capability of the PV, the ECP of the plant can range from 56% to 92% and ELCC can range from 51% to 82%. In a similar study conducted by Xcel Energy for the Public Utility Commission of Colorado, the ELCC of a 100 MW-DC PV plant located in Denver is found to be in the range of 53% to 68% (depending on sun-tracking capability), which is consistent with our results [29]. Perez et al. [10] approximate the ELCC of PV for Nevada Power (NP) and Portland General Electric (PGE) as a function of penetration using the GA method in year 2002. They assume the PV to be southwest oriented with a tilt angle of 30^{o} and fixed axis. NP is summer peaking utility with large commercial air conditioning demand. For a 2% PV penetration in NP, which is approximately equivalent to 100 MW PV capacity, they estimate the ELCC of PV to be 70%. For PGE, under a 3% penetration scenario, which is equivalent to 100 MW PV capacity, they estimate ELCC to be around 30%. The Perez et al. [10] results are significantly lower than our estimates, in Table 3, in large part due to the fact that we consider a wider footprint, which covers the entire WECC region. In contrast, Perez et al. conduct their analysis within a utility service territory or balancing area (which would be more typical of how a utility would consider the capacity value of a generation resource.) For example, while the solar resource in Portland, Oregon, in the summer appears to correlate well with the WECC-wide load, PGE was a winter peaking utility in the years analyzed by Perez et al

[11] For PV systems with either fixed-axis or single-axis tracking, tilt angle is the angle from horizontal to the inclination of the PV array. Note that tilt angle is not defined for double-axis tracking PVs.

[10], resulting in a low capacity value. As noted previously, the primary purpose of this analysis is to compare methods of capacity credit analysis.

Table 3. Average Annual Capacity Value of PV (% - Based on System AC Rating) with Fixed-Axis, Single-Axis, and Double-Axis Tracking in Different Locations

PV Site	ECP			ELCC		
	Fixed-Axis	Single-Axis Tracking	Double-Axis Tracking	Fixed-Axis	Single-Axis Tracking	Double-Axis Tracking
Bartsow, CA	64.2	78.3	79.4	59.7	72.7	73.7
Congress, AZ	75.1	82.7	85.7	69.7	76.8	79.5
Yucca Flat, NV	61.0	74.2	76.1	56.6	68.9	70.7
Hanover, NM	61.0	70.3	71.2	56.7	65.3	66.2
Cheyenne, WY	55.8	77.9	80.5	51.8	72.4	74.8
Salt Lake City, UT	65.7	84.7	88.6	61.0	78.7	82.2
Boise, ID	71.1	87.4	92.2	66.0	81.2	85.6
Los Angeles, CA	56.0	83.4	85.0	52.0	77.4	78.9
San Francisco, CA	60.1	83	84.5	55.8	77.1	78.4
Seattle, WA	62.0	87.2	92.7	57.6	80.9	86.1
Denver, CO	64.6	75.1	77.9	60.0	69.8	72.3
Albuquerque, NM	72.6	84.6	86.5	67.4	78.5	80.3
Phoenix, AZ	69.4	77.1	78.2	64.4	71.6	72.6
Las Vegas, NV	64.6	82.6	84.6	60.0	76.7	78.5

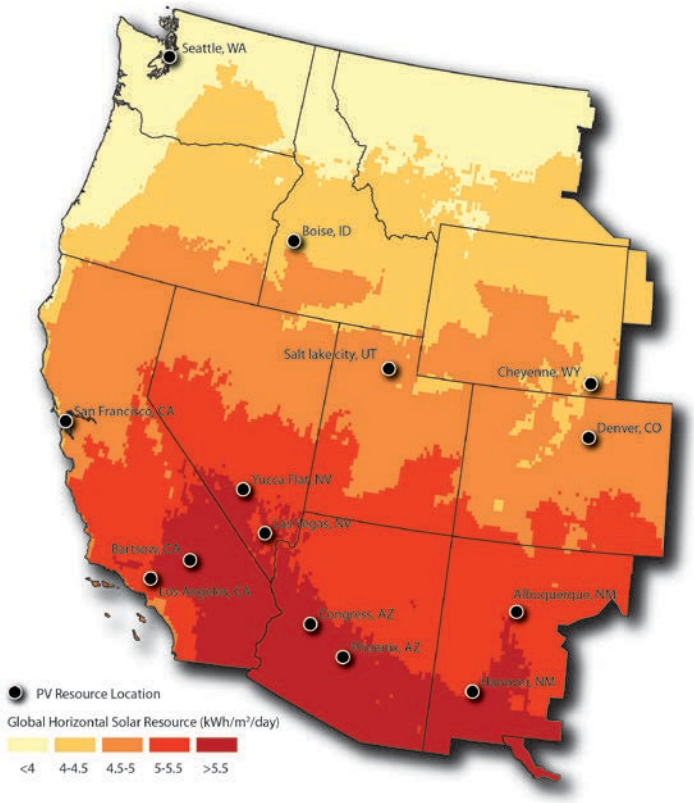

Figure 2. Location of PV sites evaluated

Because this analysis uses the same load pattern for all locations, the different ECP and ELCC values depend on the regional variation in solar resource. For instance, PV with fixed axis located in Congress, Arizona, which has a relatively high solar irradiation, has an average annual ECP of 75.1%. PV located in an urban area, such as Los Angeles, California, only has an ECP of 56%. This difference is due to lower correlation between WECC loads and PV generation in Los Angeles compared to Congress. To illustrate this, Figure 3 shows the output of a PV plant in Congress and Los Angeles on July 20, 2005. This is the day with the highest WECC-wide load of 2005. As Figure 3 shows, PV generation and load are more correlated in Congress compared to Los Angeles. In hour 14 when load reaches its annual peak, the PV in Congress is producing 66 MWh whereas the PV in Los Angeles is only producing 16 MWh. Since the capability of producing during peak load hours has a direct impact on the capacity value of a plant, one can expect that PV in Los Angeles would have a lower capacity value compared to PV located in Congress. It is important to stress that any correlation between local loads in Los Angeles and Congress and local solar resource are not captured in our analysis because we use a WECC-wide footprint.

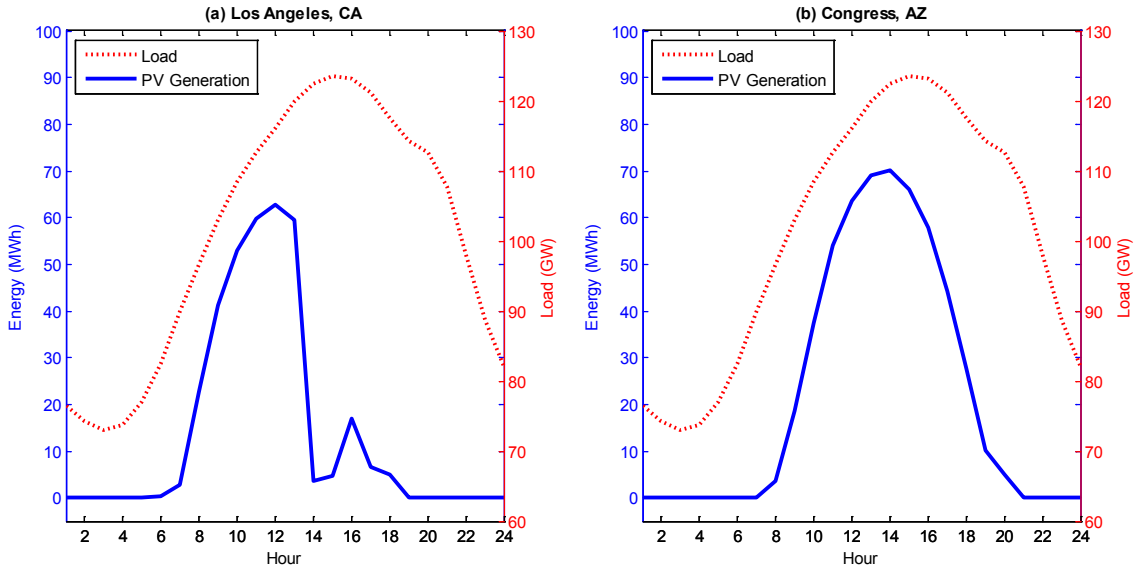

Figure 3. Hourly loads and dispatch of a fixed-axis PV plant located in Los Angeles, California, and Congress, Arizona, on July 20, 2005

As can be seen from Table 3, there are areas with high capacity values despite having a relatively low average solar resource, such as Boise, Idaho, and Seattle, Washington. These are locations in which PV generation has a relatively high correlation with the Western Interconnect loads. As expected, such a high correlation would result in higher capacity values. As an example, Figure 4 shows the output of a fixed-axis PV plant located in Boise, Idaho, and Seattle, Washington, during July 10, 2002. This is the day on which the load reaches its peak value in year 2002. The relatively high correlation between load and PV generation is observable from this figure.

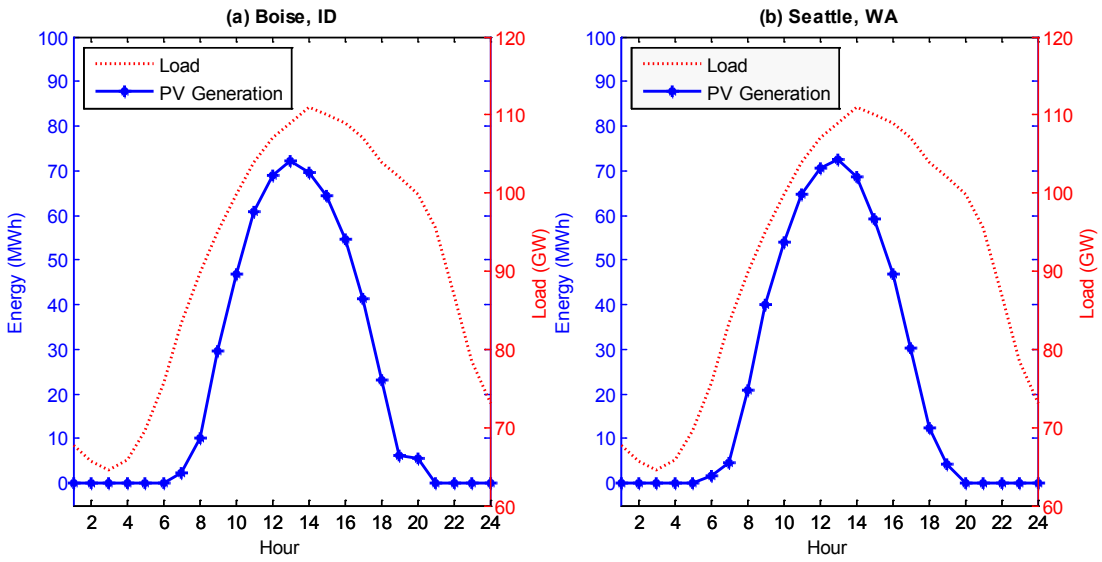

Figure 4. Hourly loads and dispatch of a fixed-axis PV plant located in Boise, Idaho, and Seattle, Washington, on July 10, 2002

The values shown in Table 3 are annual averages. We find significant interannual variation in capacity values between the years studied. This indicates that several years of data are necessary for an accurate and robust long-term estimate of capacity value (this includes both renewable supply data and conventional generator EFOR estimates). For instance, the ECP of PV in Congress, Arizona, ranges from 48% in the year 1999 to 85% in the year 2002. In each year, solar availability during peak load hours can change, which affects the capacity value of PV. To demonstrate this, Figure 5 depicts the output of a fixed-axis PV plant during July 12, 1999, and July 10, 2002. These are days on which the load reaches its peak value in the years 1999 and 2002. As Figure 5 shows, the correlation between PV generation and load is greater in the year 2002 compared to 1999. This explains the significantly greater capacity value in 2002 than in 1999.

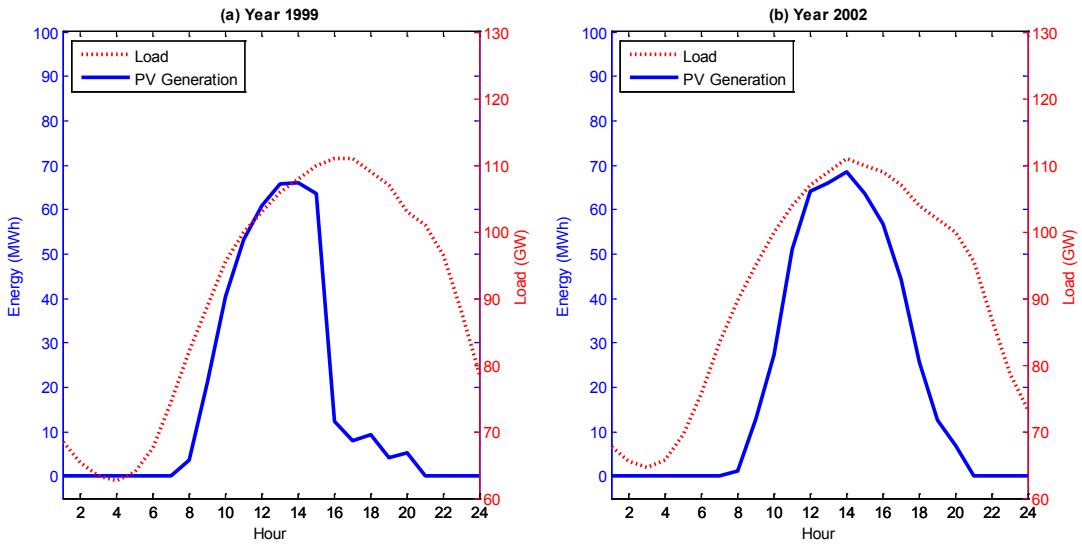

Figure 5. Hourly loads and dispatch of a fixed-axis PV plant located in Congress, Arizona, on July 12, 1999, and July 10, 2002

Although the robustness of capacity value estimates increases with more data, there is an inherent tradeoff because multiple years of accurate and time-synchronized load and solar data may be difficult to obtain. We can demonstrate the benefits of having additional load data by using a root mean squared error (RMSE) metric to measure the difference in the ECP estimated using all years of data as opposed to a subset of the data. This RMSE metric is defined as:

$$\sqrt{\frac{1}{|\Lambda|.|O|}\sum_{\lambda\in\Lambda}\sum_{o\in O}\left(ECP_{\lambda,o,Y}-ECP_{\lambda,o,Y'}\right)^2} \qquad (13)$$

where Λ is the set of locations modeled, O is the set of sun-tracking capabilities modeled (fixed-axis and single- and double-axis tracking), and $ECP_{\lambda,o,Y}$ is the ECP at location λ with sun-tracking capability o using years from dataset Y. Y is the set with all eight years and Y' is a subset of these years. Table 4 summarizes this metric for a subset of two to seven years. The RMSE is averaged over different possible sets of consecutive data that can be used.

Table 4. Average RMSE Estimates Between ECP Estimates using all Eight Years and a Subset of the Data

Years Used	RMSE
2	6.6
3	5.4
4	4
5	2.9
6	1.8
7	0.8

The table shows that having more years of data available provides more robust capacity value estimates because the RMSE decreases when more data are included in the ECP calculation. The table can further be used to measure the benefit of gathering additional data (in terms of reduced ECP error) against the cost of gathering such data and conducting additional capacity value estimation calculations.

5.2 Capacity Value of Photovoltaic Power using Approximation Techniques

This section details the capacity value of PV using the approximation techniques described in Section 2.4, using all eight years of data. Since the methods are known to be approximations of ELCC, their accuracy is compared to the actual ELCC values shown in Table 3.

5.2.1 Capacity Value of Photovoltaic Power using Capacity Factor Approximation

Although CF approximation requires an initial LOLP calculation to obtain weights, there is no need for iterative LOLP calculations. This will inevitably reduce computational time and complexity. This type of approximation is sensitive to the number of hours considered. Previous studies have shown that considering only the top 10 hours is sufficient for CSP plants [15]. We conduct a similar comparison here by considering the top 10, 100, and 10% peak-load hours and find that the top 10 hours yield approximations that are closest to the actual ELCC values. For the sake of brevity, only results regarding top 10 hours are reported in this section. Table 5 summarizes average annual capacity value of PV using CF approximation for the sites listed in Table 2.

Table 5. Average Annual Capacity Value of PV (% Based on System AC Rating) with Fixed-Axis, Single-Axis, and Double-Axis Tracking in Different Locations using CF Approximation

PV Site	Fixed-Axis	Single-Axis Tracking	Double-Axis Tracking
Bartsow, CA	60.4	71.8	75.5
Congress, AZ	70.4	77.1	79.7
Yucca Flat, NV	57.9	69.4	72.8
Hanover, NM	57.3	65.2	68.1
Cheyenne, WY	57.3	75.5	75.9
Salt Lake City, UT	67.7	81.4	84.4
Boise, ID	72.6	84.5	86.5
Los Angeles, CA	56.8	73.9	74.9
San Francisco, CA	61.2	77.0	78.4
Seattle, WA	66.2	82.8	86.0
Denver, CO	61.6	71.0	73.9
Albuquerque, NM	69.8	80.6	82.1
Phoenix, AZ	65.9	71.6	74.2
Las Vegas, NV	62.8	78.1	79.5

5.2.2 Capacity Value of Photovoltaic Power using Garver's Approximation Method

Garver's approximation for ELCC, explained in Section 2.4.2, is used to estimate capacity value of PV for years 1998–2005. Table 6 shows average annual capacity values using this method for the sites listed in Table 2.

Table 6. Average Annual Capacity Value of PV (% Based on System AC Rating) with Fixed-Axis, Single-Axis, and Double-Axis Tracking in Different Locations using GA

PV Site	Fixed-Axis	Single-Axis Tracking	Double-Axis Tracking
Bartsow, CA	58.3	73.5	75.7
Congress, AZ	62.7	73.6	75.8
Yucca Flat, NV	55.5	71.7	74.1
Hanover, NM	50.1	60.1	61.4
Cheyenne, WY	55.8	61.6	65.8
Salt Lake City, UT	60.9	69.9	71.0
Boise, ID	60.1	67.3	69.1
Los Angeles, CA	54.6	65.4	68.7
San Francisco, CA	45.0	58.6	59.8
Seattle, WA	54.7	69.1	70.6
Denver, CO	60.6	70.4	77.5
Albuquerque, NM	51.8	70.6	71.6
Phoenix, AZ	51.9	64.7	67.8
Las Vegas, NV	50.7	68.0	70.2

5.2.3 Capacity Value of Photovoltaic Power using Garver's Approximation Method for Multi-State Units

The GAM method described in Section 2.4.3 is fairly sensitive to the probability distribution utilized for PV generation. Although using an empirical distribution with a 1 MW resolution seems to be reasonable, our results show a large gap between actual ELCC values and the ones obtained from this method. Thus, GAM does not appear to be a reliable method for capacity value estimation of PV. Table 7 summarizes average annual capacity values using GAM for the sites listed in Table 2.

Table 7. Average Annual Capacity Value of PV (% Based on System AC Rating) with Fixed-Axis, Single-Axis and Double-Axis Tracking in Different Locations using GAM

PV Site	Fixed-Axis	Single-Axis Tracking	Double-Axis Tracking
Bartsow, CA	25.4	32.5	36.5
Congress, AZ	24.6	31.3	35.1
Yucca Flat, NV	25.2	32.4	36.6
Hanover, NM	24.3	30.7	34.4
Cheyenne, WY	22.1	26.0	30.2
Salt Lake City, UT	24.7	30.7	34.3
Boise, ID	23.3	29.7	32.4
Los Angeles, CA	24.0	28.7	34.0
San Francisco, CA	22.0	27.9	30.3
Seattle, WA	20.9	27.7	29.0
Denver, CO	20.6	26.2	29.2
Albuquerque, NM	23.1	30.4	32.0
Phoenix, AZ	19.9	24.1	26.6
Las Vegas, NV	14.9	19.2	20.0

In order to demonstrate the effect of how the distribution of PV availability is modeled on the GAM, we conduct a set of analyses for cases in which the empirical probability distribution is represented using a coarser resolution. We built an empirical probability distribution with 10, 20,

and 33 MW blocks by aggregating PV generation accordingly. Table 8 summarizes these results for PV plants with fixed-axis. PV plants with tracking systems have similar results.

Table 8. Average Annual Capacity Value of PV (% Based on System AC Rating) with Fixed-Axis in Different Locations using GAM Assuming PV Probability Distribution with 1, 10, 20, and 33 MW Resolution

PV Site	1 MW Res.	10 MW Res.	20 MW Res.	33 MW Res.
Bartsow, CA	25.4	34.8	43.9	57.6
Congress, AZ	24.6	33.9	43.6	56.5
Yucca Flat, NV	25.2	34.6	44.0	57.2
Hanover, NM	24.3	33.6	43.1	56.2
Cheyenne, WY	22.1	31.5	40.9	54.7
Salt Lake City, UT	24.7	34.0	43.2	57.1
Boise, ID	23.3	32.6	42.5	54.9
Los Angeles, CA	24.0	33.3	42.9	55.7
San Francisco, CA	22.0	31.3	40.8	54.5
Seattle, WA	20.9	30.1	40.0	53.0
Denver, CO	20.6	30.0	39.7	53.1
Albuquerque, NM	23.1	32.4	41.3	55.7
Phoenix, AZ	19.9	29.2	38.8	52.3
Las Vegas, NV	14.9	24.2	33.9	48.3

5.2.4 Capacity Value of Photovoltaic Power using the Z Method

Table 9 summarizes average annual capacity values using the Z method for the sites listed in Table 2.

Table 9. Average Annual Capacity Value of PV (% Based on System AC Rating) with Fixed-Axis, Single-Axis, and Double-Axis Tracking in Different Locations using the Z Method

PV Site	Fixed-Axis	Single-Axis Tracking	Double-Axis Tracking
Bartsow, CA	46.8	67.6	68.4
Congress, AZ	61.8	77.9	79.2
Yucca Flat, NV	44.5	68.9	69.9
Hanover, NM	48.4	64.5	65.1
Cheyenne, WY	46.8	61.2	61.7
Salt Lake City, UT	52.4	63.9	64.9
Boise, ID	56.6	67.1	67.3
Los Angeles, CA	49.5	72.6	72.7
San Francisco, CA	53.4	71.2	71.9
Seattle, WA	62.2	76.1	76.5
Denver, CO	66.6	78.3	79.3
Albuquerque, NM	52.6	69.5	70.6
Phoenix, AZ	58.3	73.3	74.4
Las Vegas, NV	60.2	80.1	81.3

5.2.5 Comparison Between Different Approximation Techniques

In order to understand the accuracy of each of the approximation techniques, we use an RMSE metric. The RMSE metric is defined as:

$$\sqrt{\frac{1}{|\Lambda|.|O|}\sum_{\lambda\in\Lambda}\sum_{o\in O}\left(ELCC_{\lambda,o}-A_{\lambda,o}\right)^2} \qquad (14)$$

where Λ is the set of locations modeled, O is the set of tracking capabilities modeled (fixed-axis and single- and double-axis tracking), $ELCC_{\lambda,o}$ is the ELCC at location λ with tracking capability o, and $A_{\lambda,o}$ is the approximation method used at location λ with tracking capability o. Table 10 rank orders different approximation techniques based on this metric.[12] According to Table 10, CF approximation yields the closest approximations to ELCC and GAM_1 is the least accurate in this manner.

Table 10. Average RMSE of ELCC for Different Approximation Techniques

Approximation Technique	RMSE
CF	4.12
GA	11.9
Z	13.5
GAM_33	14.9
GAM_20	25.8
GAM_10	34.4
GAM_1	44.4

[12] GAM_1, GAM_10, GAM_20, and GAM_33 refer to the GAM method assuming an empirical PV probability distribution with 1, 10, 20, and 33 MW resolutions, respectively.

6 Sensitivity Analysis

This section examines the sensitivity of changes in PV orientation and the inverter model on capacity value.

6.1 Sensitivity of Capacity Value of Photovoltaic Power with Respect to Array Orientation

The results reported in Section 5 were under the assumption that the PV array is oriented to face south (azimuth angle of 0) and tilt angle equivalent to the latitude of the site. Changing the orientation of the PV array would affect both the energy yield and capacity value. An azimuth angle of zero typically maximizes energy yield [33]. In the northern hemisphere, increasing the azimuth angle will favor afternoon energy production and decreasing it will favor morning energy production.

The ability of a generator to produce energy during peak load hours directly impacts its capacity value. All of the sites considered in this study are located in the western United States where load tends to peak in summer afternoons. As a result, an increased azimuth angle tends to increase energy production in the afternoon and potentially increase capacity value but with the penalty of decreased energy yield. We examine this effect by estimating the capacity value and annual energy yield for four sites—Bartsow, California, Congress, Arizona, Yucca Flat, Nevada, and Hanover, New Mexico—as a function of azimuth and tilt angles. Note that we use ECP as an estimate for capacity value and we also assume that the PV is fixed-axis. We define the azimuth angle as ranging from -90 (facing east) to 90 (facing west) with 0 facing due south and sweep over these angles in 10-degree increments. However, we only report results for azimuth angles ranging from 0 to 90 because systems facing toward east are not efficient in terms of capacity value and energy yield.

Figure 6 depicts the average capacity value and annual energy yield as a function of azimuth and tilt angles for a site located in Bartsow, California, with coordinates shown in Table 2. Figure 6 shows that some orientations yield to a capacity value greater than 100%. As explained in Section 3, capacity values are normalized by the STC AC capacity of the PV plant, which we find to be 83.4 MW. This is not necessarily the maximum AC output of the PV, and depending on solar irradiance and cell temperature, it is possible for the PV plant to generate more than 83.4 MW.

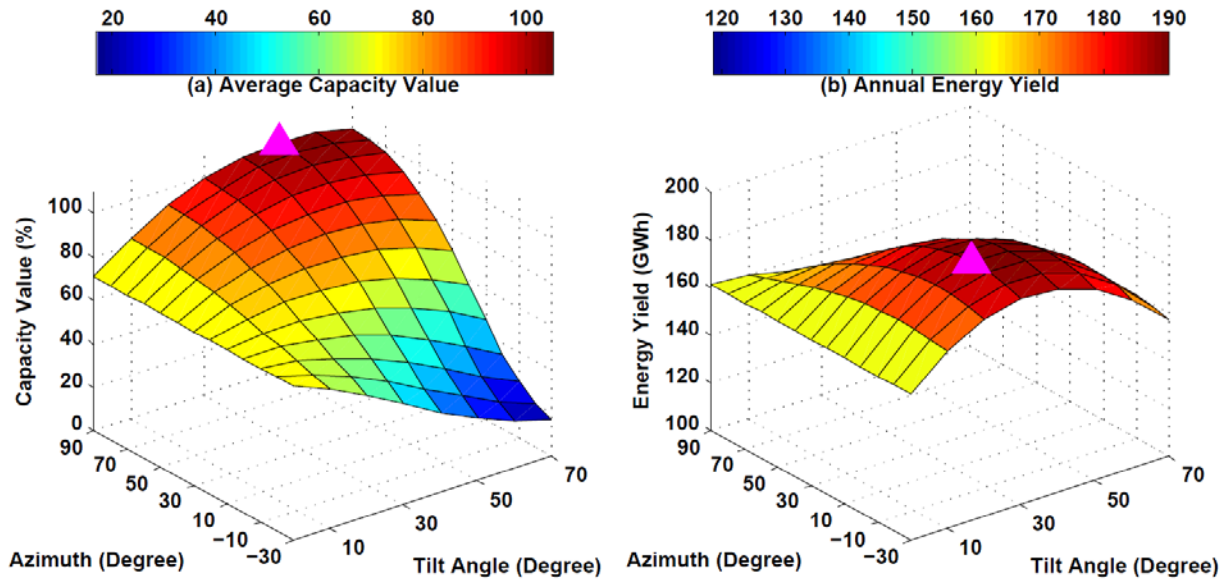

Figure 6. Average annual capacity value and energy yield of PV at Bartsow, California, as a function of azimuth and tilt angles. Magenta triangles show the maximum.

Figure 7 depicts the average capacity value and annual energy yield as a function of azimuth and tilt angles for a site located in Congress, Arizona, with coordinates shown in Table 2.

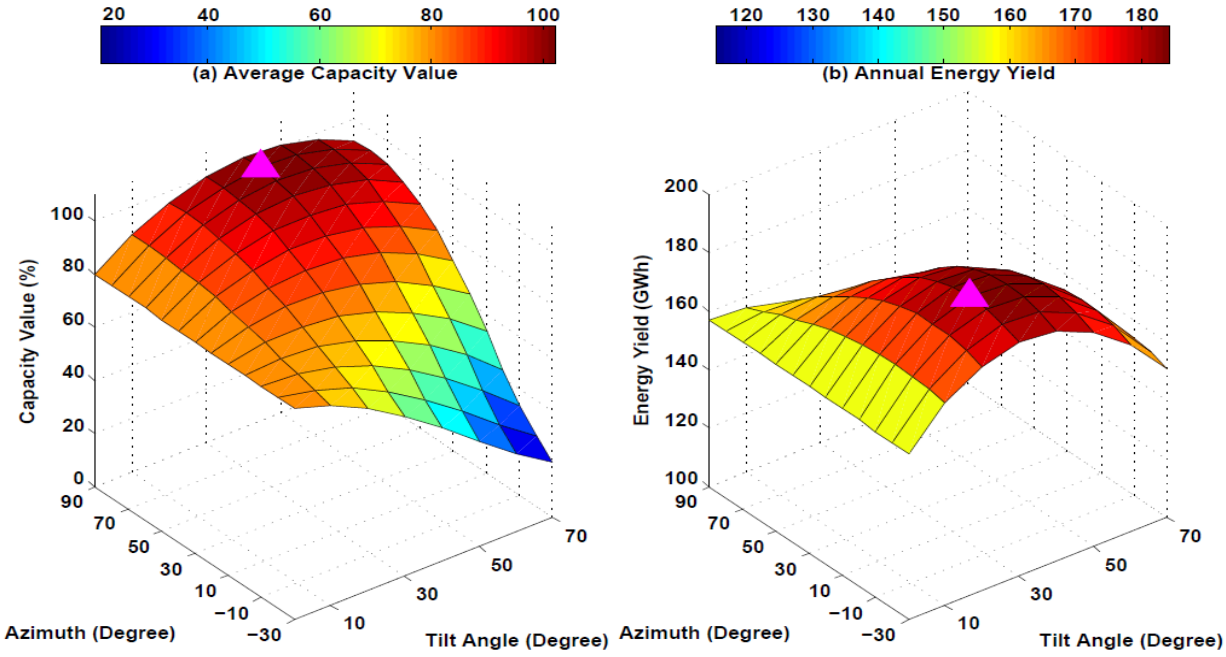

Figure 7. Average annual capacity value and energy yield of PV at Congress, Arizona, as a function of azimuth and tilt angles. Magenta triangles show the maximum.

Figure 8 depicts the average capacity value and annual energy yield as a function of azimuth and tilt angles for a site located in Yucca Flat, Nevada, with coordinates shown in Table 2.

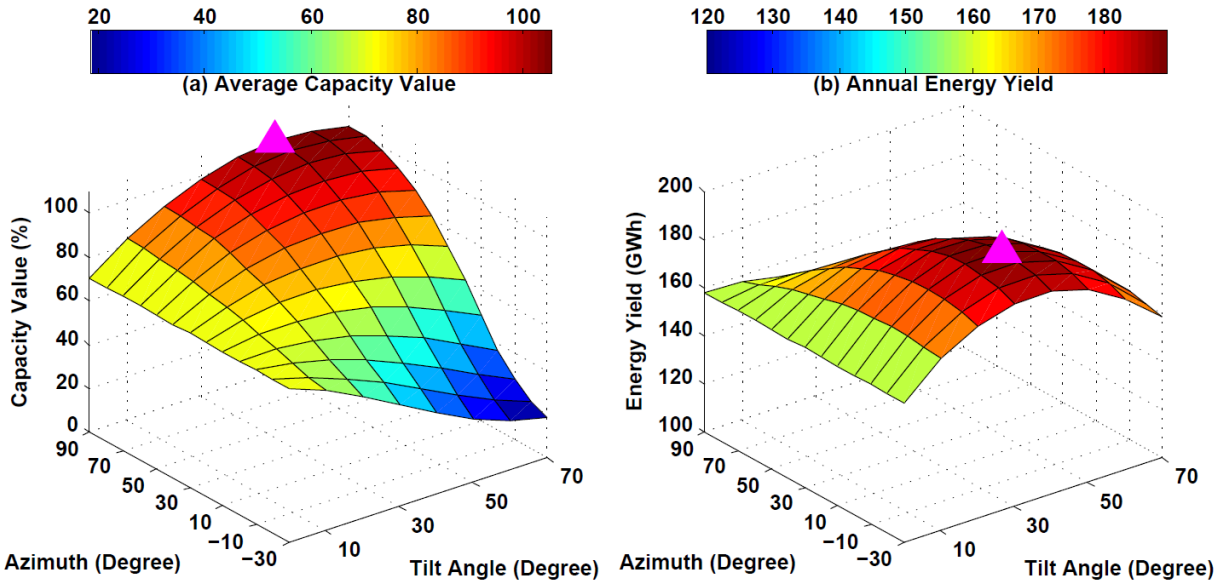

Figure 8. Average annual capacity value and energy yield of PV at Yucca Flat, Nevada, as a function of azimuth and tilt angles. Magenta triangles show the maximum.

Figure 9 depicts the average capacity value and annual energy yield as a function of azimuth and tilt angles for a site located in Hanover, New Mexico, with coordinates shown in Table 2.

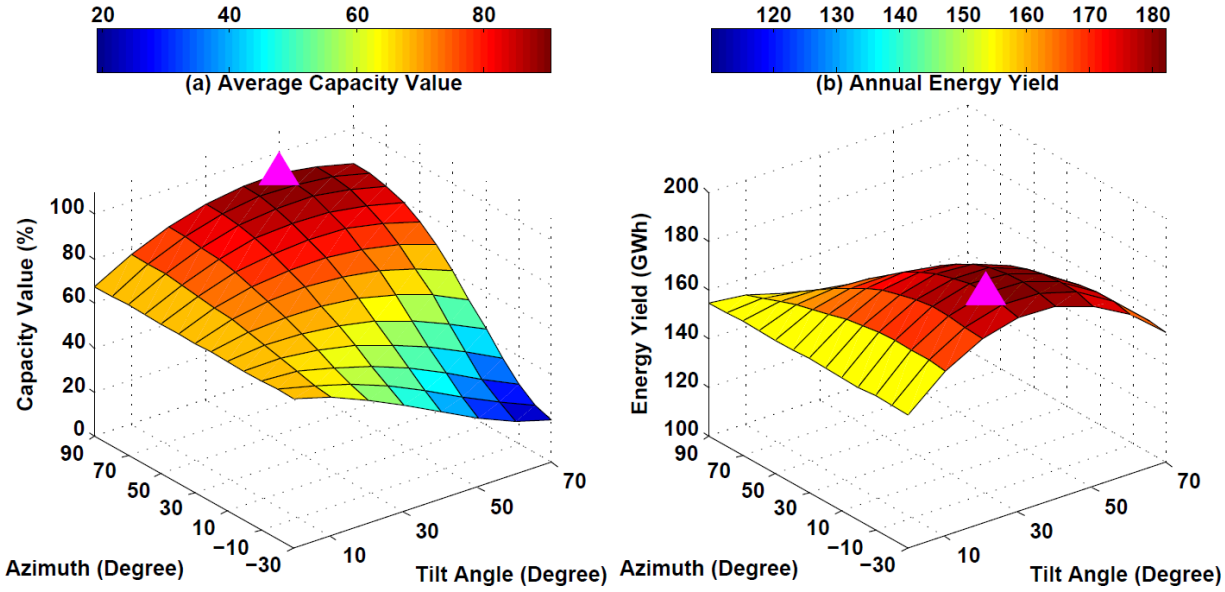

Figure 9. Average annual capacity value and energy yield of PV at Hanover, New Mexico, as a function of azimuth and tilt angles. Magenta triangles show the maximum.

As expected, Figures 6–9 reveal a tradeoff between capacity value and energy yield. Capacity value increases with azimuth angle while the reverse is true for annual energy yield. Therefore,

the orientation of PV array represents a tradeoff driven by market conditions including the presence of energy or capacity markets and other incentives for energy production. Table 11 summarizes the orientations that maximize average annual capacity value and annual energy yield for the four locations analyzed in Figures 6–9. The maximum average annual capacity value and annual energy yield are also identified in Table 11. As shown in the table, orientations that maximize annual capacity value and energy yield are similar with respect to the tilt angle; they differ at most by 20 degrees. However, the azimuth angles are significantly different showing the tradeoff between capacity value and energy yield.

Table 11. Orientation that Maximizes Average Annual Capacity Value and Annual Energy Yield Along with Maximum Average Annual Capacity Value (%) and Energy Yield (GWh) in Different Locations

PV Site	Capacity Value		Energy Yield	
	Maximum Value (%)	Orientation (Azimuth,Tilt)	Maximum Value (GWh)	Orientation (Azimuth,Tilt)
Bartsow, CA	105.0	(90^o,50^o)	190.0	(0^o,30^o)
Congress, AZ	102.2	(80^o,40^o)	184.2	(0^o,30^o)
Yucca Flat, NV	105.3	(90^o,50^o)	189.2	(0^o,40^o)
Hanover, NM	90.5	(90^o,50^o)	181.8	(-10^o,30^o)

6.2 Sensitivity of Capacity Value of Photovoltaic Power with Respect to Inverter Model

The SIPM used throughout our analysis has a non-linear behavior, which is depicted in Figure 1. The inverter is more efficient at higher power outputs. Simpler single point efficiency inverter models (SPEIM) are occasionally used to model PV systems. If the single efficiency used in a SPEIM is properly set, the total simulated energy yield over the year can closely match the result of using a SIPM. This is because the inverter efficiency will be over- and under-estimated in some hours but will balance each other out over the course of the year. Using an SPEIM can introduce significant errors when estimating the capacity value of PV, however, because the capacity value is highly sensitive to the timing of PV output. In order to demonstrate this, we substitute the SIPM used in our analysis with an SPEIM with a 94% efficiency, based on the default value in SAM. Table 12 summarizes the average annual change in ECP of PV plants as a result of this substitution.

Table 12. Average Annual Change in Capacity Value when SPEIM is Utilized as Opposed to SIPM for Fixed-Axis, Single-Axis, and Double-Axis Tracking PVs in Different Locations

PV Site	Fixed-Axis	Single-Axis Tracking	Double-Axis Tracking
Bartsow, CA	-3.2	3.4	1.5
Congress, AZ	0	3.9	3.0
Yucca Flat, NV	-2.1	3.8	3.1
Hanover, NM	-0.5	5.4	3.0
Cheyenne, WY	-3.8	3.8	3.2
Salt Lake City, UT	-5.0	0.6	1.8
Boise, ID	-5.1	0	1.8
Los Angeles, CA	-3.6	8.7	8.0
San Francisco, CA	-4.1	4.9	3.3
Seattle, WA	-7.5	1.5	4.0
Denver, CO	-2.0	2.0	2.2
Albuquerque, NM	-2.3	2.8	1.2
Phoenix, AZ	-1.2	2.3	1.0
Las Vegas, NV	-6.5	1.4	-0.4

Table 12 shows that for PV with fixed-axis, SPEIM yields a higher capacity value, whereas SIPM yields a higher capacity value when PV is equipped with a double-axis tracking system. The reason is due to the non-linear behavior of SIPM. For lower power outputs, as for the case with fixed-axis, SPEIM has higher efficiency compared to SIPM, whereas the reverse is true for high power outputs. This is because the SPEIM uses an average efficiency, which will understate inverter efficiency at high output levels and overstate it at lower levels.

7 Conclusions

This study compares several approaches for estimating the capacity value of PV. It applies these methods at a variety of locations within WECC during the years 1998–2005, while assuming the load is fixed to evaluate the variation in performance based on the solar resource. This is done by simulating hourly PV generation and using it as an input for reliability-based methods and approximation techniques that quantify capacity value. While ECP and ELCC are well recognized and widely used due to their robustness, we find that some approximation techniques can yield similar results. Our results show that PV, on average, can have ECPs between 61% and 92% and ELCCs between 52% and 86%, depending on the location and sun-tracking capability of the plant and using the system's AC rating. PV plants with two-axis tracking have the highest capacity value. Similar to other renewable resources, we find high interannual variation (±16%), indicating that multiple years of data are required for a robust estimation of capacity value. Out of the approximation techniques that we study, we find the CF approximation to be the most dependable technique, followed by GA, Z method, and GAM. We show this by rank ordering these techniques by means of an RMSE metric compared to an actual ELCC calculation.

Our analysis also examines the sensitivity of the capacity value of PV with respect to orientation and inverter model. By calculating ECP as a function of azimuth and tilt angles, we recognize a tradeoff between capacity value and annual energy yield. Orienting PV arrays toward the west favors afternoon energy production and therefore maximizes capacity value, at the expense of reduced annual energy yield. We also study the effect of inverter efficiency on ECPs. We compare average annual ECPs of PV with two different inverter models, SIPM and SEIPM. We find that for PV plants with fixed-axis, simulating PV generation with SEIPM will overestimate capacity value, while for PV plants with double-axis tracking, simulating PV generation with SEIPM will underestimate capacity value.

References

[1] "Methods to Model and Calculate Capacity Contributions of Variable Generation for Resource Adequacy Planning." North American Reliability Corporation, March 2011. http://www.nerc.com/docs/pc/ivgtf/IVGTF1-2.pdf.

[2] Pudaruth, G.R.; Li, F. "Capacity Credit Evaluation: A Literature Review." *Third International Conference on Electric Utility Deregulation and Restructuring and Power Technologies, DRPT 2008, Nanjing, China;* pp. 2719–2724.

[3] Milligan, M. "Measuring Wind Plant Capacity Value." NREL/TP-441-20493. Golden, CO: National Renewable Energy Laboratory, 1996.

[4] Milligan, M.; Factor, T. "Optimizing the Geographic Distribution of Wind Plants in Iowa for Maximum Economic Benefit and Reliability." *Wind Engineering* (24); pp. 271–290, July 2000.

[5] Milligan, M.; Parsons, B. "A Comparison and Case Study of Capacity Credit Algorithms for Intermittent Generators." *Proceedings Solar '97; April 27–30, 1997, Washington, D.C.* NREL/CP-440-22591. Golden, CO: National Renewable Energy Laboratory, March 1997.

[6] Ensslin, C.; Milligan, M.; Holttinen, H.; O'Malley, M.; Keane, A. "Current Methods to Calculate Capacity Credit of Wind Power, IEA Collaboration." *Proceedings 2008 IEEE Power & Energy Society General Meeting;* 2008, p. 3.

[7] Amelin, M. "Comparison of Capacity Credit Calculation Methods for Conventional Power Plants and Wind Power." *IEEE Trans. Power Syst.* (24:2), May 2009.

[8] Keane, A.; Milligan, M.; DAnnunzio, C.; Dent, C.J.; Dragoon, K.; Hasche, B.; Holttinen, H.; Samaan, N.; S¨oder, L.; O'Malley, M. "Capacity Value of Wind Power." *IEEE Trans. Power Syst.* (26:2), 2011; pp. 564–572.

[9] Pelland, S.; Abboud, I. "Comparing Photovoltaic Capacity Value Metrics: A Case Study for the City of Toronto." *Progress in Photovoltaics: Research and Applications* (16), December 2008; pp. 715–724.

[10] Hoff, T.; Perez, R.; Ross, J.P.; Taylor, M. "Photovoltaic Capacity Valuation Methods." SEPA REPORT # 02-08. Washington, DC: Solar Electric Power Association, 2008.

[11] Perez, R.; Kmiecik, M.; Schlemmer, J.; Root, L.; Moore, K.; Stackhouse, P. "Evaluation of PV Generation Capacity Credit Forecast on Day-Ahead Utility Markets." *Proc. ASES Annual Meeting,* Cleaveland, OH, 2007.

[12] Perez, R.; Seals, R.; Stewart, R. "Assessing the Load Matching Capability of Photovoltaics for U.S. Utilities Based Upon Satellite-Derived Insolation Data." in *Proc. 23rd IEEE Photovoltaic Specialists Conf.*, May 1993; pp. 1146–1151.

[13] Perez, R.; Margolis, R.; Kmiecik, M.; Schwab, M.; Perez, M. "Update: Effective Load Carrying Capability of Photovoltaics in the United States." *Proc. ASES Annual Meeting*, Denver, CO, 2006.

[14] Perez, R.; Seals, R.; Herig, C.; "Determination of the End-Use Effective Capacity of Photovoltaics." *Proc. 14th European PV Conference*, Barcelona, Spain, 1997.

[15] Madaeni, S.H.; Sioshansi, R.; Denholm, P. "Capacity Value of Concentrating Solar Power Plants." NREL/TP-6A20-51253. Golden, CO: National Renewable Energy Laboratory, 2011.

[16] Billinton, R.; Allan, R. *Reliability Evaluation of Power Systems*. 2nd edition. New York: Plenum Press, 1984.

[17] Kahn, E.P. "Effective Load Carrying Capability of Wind Generation: Initial Results with Public Data." *The Electricity Journal* (17:10), December 2004; pp. 85–95.

[18] Holttinen, H.; Lemstrom, B.; Meibom, P.; Bindner, H.; Orths, A.; van Hulle, F.; Ensslin, C.; Hofmann, L.; Winter, W.; Tuohy, A.; O'Malley, M.; Smith, P.; Pierik, J.; Tande, J.O.; Estanqueiro, A.; Ricardo, J.; Gomez, E.; Soder, L.; Strbac, G.; Shakoor, A.; Smith, J.C, Parsons, B.; Milligan, M.; Wan, Y. "Design and Operation of Power Systems with Large Amounts of Wind Power." VTT Working Papers 82, 2007.

[19] Garver, L.L. "Effective Load Carrying Capability of Generating Units." *IEEE Trans. on PAS* (PAS-85), August 1966; pp. 910–919.

[20] Dragoon, K.; Dvortsov, V. "Z-Method for Power System Resource Adequacy Applications." *IEEE Transactions on Power Systems* (21), May 2006; pp. 982–988.

[21] Milligan, M.; Parsons, B. "A Comparison and Case Study of Capacity Credit Algorithms for Wind Power Plants." *Wind Energy* (23:3), 1999; pp. 159–166.

[22] Haslett, J.; Diesendorf, M.; "The Capacity Credit of Wind Power: A Theoretical Analysis." *Solar Energy* (26), 1981; pp. 391–401.

[23] Soder, L.; Bubenko, J. "Capacity Credit and Energy Value of Wind Power in Hydro-Thermal Power System." *Proc. of the 9th Power Systems Computation Conference*, Cascais, Portugal, 30 August-4 September 1987.

[24] Bernow, S.; Biewald, B.; Singh, D. "Modelling Renewable Electric Resources: A Case Study of Wind Reliability." Presented at the NARUC-DOE National Conference on Renewable Energy; Savannah, GA, October 1993.

[25] El-Sayed, M. "Substitution Potential of Wind Energy in Egypt." *Energy Policy* (30), 2002; pp. 681–687.

[26] D'Annunzio, C.; Santoso, S. "Noniterative Method to Approximate the Effective Load Carrying Capability of a Wind Plant." *IEEE Trans. Energy Conv.* (23:2), June 2008; pp. 544–550.

[27] Zachary, S.; Dent, C. "Probability Theory of Capacity Value of Additional Generation." *Journal of Risk and Reliability* (226), 2012; pp. 33–43.

[28] Gilman, P.; Blair, N.; Mehos, M.; Christensen, C.; Janzou, S. *Solar Advisor Model User Guide for Version 2.0.* NREL/TP-670-43704. Golden, CO: National Renewable Energy Laboratory, August 2008.

[29] "An Effective Load Carrying Capability Analysis for Estimating the Capacity Value of Solar Generation Resources on the Public Service Company of Colorado System." Xcel Energy Services, Inc., February 2009.

[30] U.S. Department of Energy Form 860, http://www.eia.doe.goc/cneaf/electricity/page/eia860.html.

[31] North American Electric Reliability Corporation Generating Availability Data System, http://www.nerc.com/page.php?cid=4|43.

[32] Federal Energy Regulatory Commission Form No. 714, http://www.ferc.gov/docs-filing/forms/form-714/elec-subm-soft.asp.

[33] Christensen, C.B.; Barker, G.M. "Effects of Tilt and Azimuth on Annual Incident Solar Radiation for United States Locations." In *Proceedings of Solar Forum, American Society of Mechanical Engineers*, 2001; pp. 1–8.

COMMONWEALTH OF KENTUCKY

BEFORE THE PUBLIC SERVICE COMMISSION

In the Matters of:

ELECTRONIC APPLICATION OF KENTUCKY UTILITIES COMPANY FOR AN ADJUSTMENT OF ITS ELECTRIC RATES, A CERTIFICATE OF PUBLIC CONVENIENCE AND NECESSITY TO DEPLOY ADVANCED METERING INFRASTRUCTURE, APPROVAL OF CERTAIN REGULATORY AND ACCOUNTING TREATMENTS, AND ESTABLISHMENT OF A ONE-YEAR SURCREDIT	)	CASE NO. 2020-00349
ELECTRONIC APPLICATION OF LOUISVILLE GAS AND ELECTRIC COMPANY FOR AN ADJUSTMENT OF ITS ELECTRIC AND GAS RATES, A CERTIFICATE OF PUBLIC CONVENIENCE AND NECESSITY TO DEPLOY ADVANCED METERING INFRASTRUCTURE, APPROVAL OF CERTAIN REGULATORY AND ACCOUNTING TREATMENTS, AND ESTABLISHMENT OF A ONE-YEAR SURCREDIT	)	CASE NO. 2020-00350

AFFIDAVIT OF JUSTIN BARNES
VERIFICATION

JURISDICTION)
)
County of Wise, Virginia)

The undersigned, Justin Barnes, being first duly sworn, states the following: The prepared Responses to Commission Staff attached thereto constitute the testimony of Affiant in the above-styled cases. Affiant states that he would give the answers set forth in the Responses if asked the questions propounded therein. Affiant further states that, to the best of his knowledge, his statements are true and correct. Further, Affiant saith not.

Name of Witness

SUBSCRIBED AND SWORN to before me on this 2nd day of August, 2021 by John Barnes

Mary Lee Hagy
NOTARY PUBLIC

My Commission Expires: 06/30/2023